31st Congress of the International Council of the Aeronautical Sciences

Belo Horizonte, Brazil; September 09-14, 2018

PARAMETRIC INVESTIGATION OF EESC-USP AEROACOUSTIC FAN RIG

Rafael Gigena Cuenca* , **Paulo Celso Jr.**** , **Bernardo Martinez Rocamora****
***Federal University of Santa Catarina** , ****University of São Paulo**

Keywords: *Aeroacoustics, Turbofan Noise, Metamodel, Kriging Method, Parametric Analysis*

Abstract

In July 2016, a parametric campaign was conducted at the EESC-USP low speed Fan Rig. In it, was changed the parameters: shaft speed, rotor-stator spacing and throttling. Over these parameters were calculated the variables axial Mach velocity, blade tip Mach number, advance ratio J. The noise is defined over a parametric curve fitted on spectra and a kriging surface regression was used to better observe the noise parameter trends. The broadband noise level increase with axial mach and mach tip, as expected. The increase of RSS causes a reduction of BB decay. The tones are modeled as exponential decay (in tonal order), the first tonal level tends to decrease with advanced ratio, axial mach and RSS. Its decay has a soft tendency to increase with RSS and decrease with axial Mach and J.

1 INTRODUCTION

Over the last decades, the air transport operating cost and increasing demand for long range fast transport has made the very large aircraft more popular, for cargo and passengers. That increase in payload associated with the growth in airport traffic tends to increase airport noise levels. At the same time, the aeronautical authorities have been, gradually, restricting the acceptable noise levels. The first approach on aircraft noise reduction was applied to jet engines and that was achieved by the high bypass turbofan engines. In that way, others sources of noise of the airplane increased on importance ranks. A good review of aircraft noise is presented on Ref.[1].

As a consequence of the reduction of the major noise sources on the airplane, the engine noise is increasing again in importance, especially the noise related to the fan of the high bypass engine [2]. The noise related to the fan is a consequence of the turbulent wake of rotor impinging on the stator vane, resulting in broadband (BB) and tonal noise (BPF). The localization of the main noise sources is on leading and trailing edge of blades and vanes, being the vane's leading edge the one most influenced by wake interaction.

The experimental investigations on turbofan engines are the focus of many research teams and the industry. In the industry, real engine parts can be used in the tests and, in the academy, scaled models are used more often, even to measure the spectra or modal structure of the in-duct noise. In Ref.[3] shows a rotating rake used to perform the modal decomposition in full scale and scaled models. At academy there are some examples of aeroacoustic fan rigs [3, 4, 5, 6, 7, 8, 9, 10], that can be classified as short duct or long duct.

To allow the investigation of noise behavior, a test campaign was conducted at the EESC-USP Aeroacoustic Fan Rig, shown on Fig. 1 and described on Ref.[10]. That equipment has a fan model with the same geometry of the fan aeroacoustic test bed at NASA Glenn [3], with 16 blades and 14 vanes. The rig has the means to change the RSS and a throttling device is used to control the mass flow for different shaft speeds. The throttle is a simple flow obstruction with a defined blocked area, according to the ISO-5136

standard [11].

Fig. 1 EESC-USP Aeroacoustic Fan Rig.

The parametric campaign was conducted in July 2016 and the shaft speeds were: 3000, 3200, 3500, 3700, 4000 and 4250. The RSS, as a fraction of blade chord, used on tests were: 0.43, 0.95 and 1.48. The throttle is defined as a fraction of blocked areas and the following values were used on tests: 0%, 24.3%, 37.7% and 52.2%.

2 Data Fitting and Regression

The data analysed was the average in-duct autospectra measured by 14 microphones. An example of that spectrum, been the frequency normalized by shaft frequency, is shown in Fig. 2 and the broadband and tonal components of noise can be noted and it is observed, on linear scale of frequency, a broadband with a practically linear decay. For some of the spectra observed, the decay behavior diverts from linear, so a form factor is used on the broadband parametric curve. This parameterization is defined by:

$$BB(f) = L_p - A * f^b + \sum_{k=1}^{n} \alpha_k e^{\left(\frac{f-kf_b}{\sigma_b}\right)^2} \qquad (1)$$

where L_p is the BB level (dBs), A is the linear decay ($dBs/(Hz/\Omega)$), b is the form factor and f is the frequency normalized by the shaft speed. For form factor $b = 1$ the BB is linear, for $b > 1$ the BB curves down at high frequencies and for $b < 1$ the curves up at high frequencies. σ_b is the tonal width, adopted as 0.5. The summation computes the tones represented by gaussians, been f_b the BPF frequency and α_k the intensity of tone above BB and it behavior are exponential with frequency. Because the frequency is normalized, the BPFs will always be multiples of B (blades count). To define the BPF model, a first fitting is performed on each tonal level above the BB and then an exponential curve fitting is performed in the BPF levels for each spectrum. The fitting is performed using a non-linear least square method, with no user inputs. The relation between the spectrum parameters and the rig variables are investigated using a kriging surface regression [12] to make clear the function behavior.

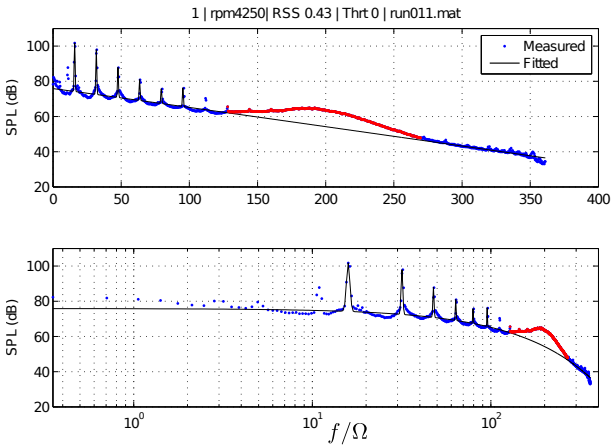

Fig. 2 In-Duct measured Noise and Parametrization Curve.

3 Experimental Result and Analysis

The aerodynamic data of the internal flow of the rig were measured using a micronamometer and a static pitot tube. The atmospheric data, as temperature and pressure, was measured using a portable meteorological station. This allowed the calculation of flow speed and sound speed.

The use of the throttling device allows the control of fan advance ratio, define by:

$$J = \frac{V_a}{\Omega D} \qquad (2)$$

been V_a the fan's axial air speed, Ω is the shaft speed and D the fan diameter. Fig. 3 shows the

advance ratio for different configurations of the fan, calculated using Eq.2. First, it is possible to see, with all the bars with the same colors having the same height, that the axial speed of the flow adjusts itself so that the advance ratio is maintained constant with the rotational speed changes. This justifies the use of advance ratio instead of throttling configuration or area restriction at the outlet of the Rig. It is also possible to see that the rotor-stator spacing (RSS) has almost no effect on the advance ratio, since the three blocks of bars are almost equal.

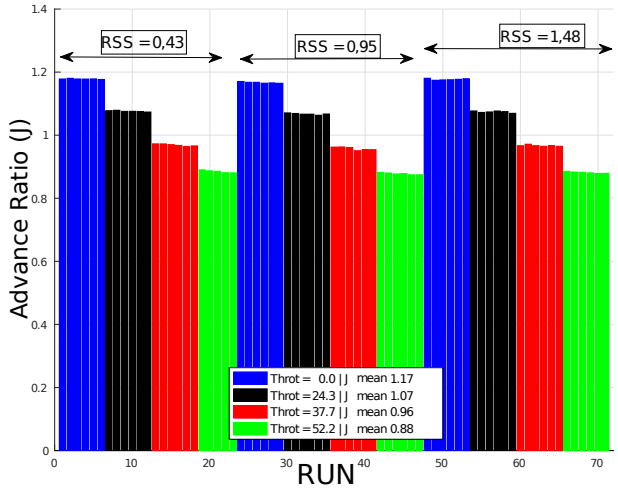

Fig. 3 Fan advance ratio J for different shaft speed (each of the bars), throttling configurations (each of the colors) and RSS (each of three groups).

The Advance Ratio presented on Fig. 3 are related only with cases that the fan is not stalled. Using the data of stalled fan (throttle configuration with higher flow obstruction) it is possible to see in Fig. 4 that the advance ratio has not a linear relation with outlet area. But, as for the small relative outlet area configurations and logarithm regression shows a good trend.

The relationship between shaft speed and Mach number allows a calibration of the Rig, as well made on Ref.[13]. The analysis of the data obtained in the parametric campaign shows that this calibration is not quite affected by the RSS. However, it is possible to obtain a calibration value for each throttling configuration using a linear regression method (Fig. 5).

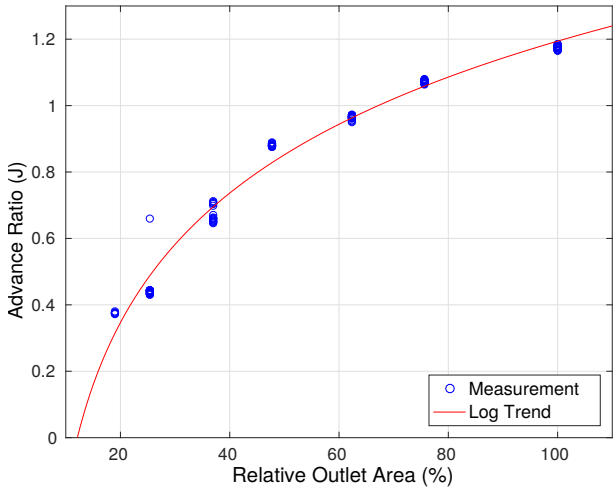

Fig. 4 Fan advance ratio J for different relative output area.

3.1 Broadband Noise Level

Aiming to better visualize the tendencies on broadband level, a Kriging regression is applied to construct a surface formed by the axial and blade tip Mach number, advance ratio and RSS data. The results are seen on Fig. 6, Fig. 7 and Fig. 8. The colors on the surface represents the estimated error of the regression. Obviously, the regions with lack of sampling, the errors are greater (in yellow) and the tendency is not achieved.

On Fig. 6, it is possible to note the increase of broadband with the advance ratio reduction. This is the expected effect since the reduction in the advance ratio means that there is an increase in blade loading. At the lowest and highest velocities, the regression does not maintain its tendency, so more data is needed to represent the noise behavior.

Fig. 7 compares the blade tip Mach number. It is possible to see that there is tendency of SPL to reduce for averages values of J and that the increase of the broadband level with tip Mach is maintained with less data dispersion.

Fig. 8 shows the regression of the RSS and axial Mach number. It points out to a small decrease in the broadband level with increase in RSS.

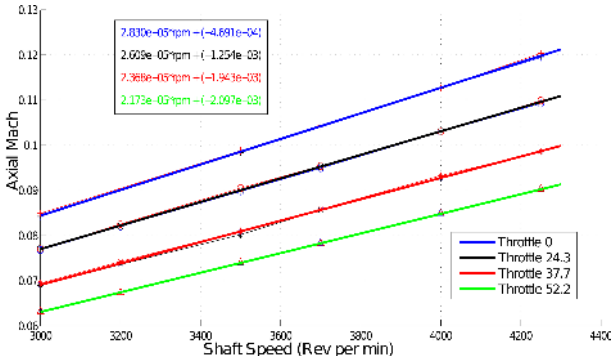

Fig. 5 Linear regression of shaft speed effect on axial Mach number.

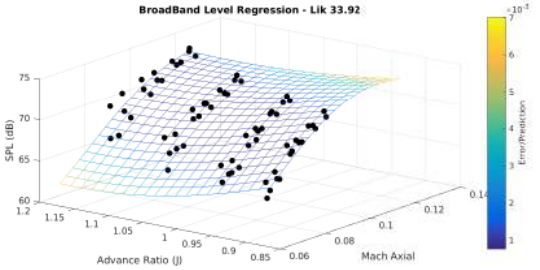

Fig. 6 Kriging regression: J and axial Mach number effect on broadband level.

3.2 Broadband Noise Decay

It was perceptible that the broadband level decays with frequency, hence it was modeled with a linear behavior to represent its decay. Fig. 9 shows that the broadband decay is very dependent on the rotational speed for the smallest RSS configuration and becomes less sensitive as the RSS increased, in a manner that it is almost not affected by the shaft speed for the configuration with larger RSS.

Fig. 10 shows again that the decay factor decreases with the increase in RSS, but also indicates that this effect is stronger for lower axial Mach numbers, where the decay drops by one decade in dB/Hz. Fig. 11 analyses the same effect, but for the tip blade mach number. Again, as the RSS is diminished, the decay factor is decreased. Now, the data is better distributed and the surface has lower error on its boundaries. The decay drops up to almost two decades for larger RSS and lower tip blade Mach number configuration.

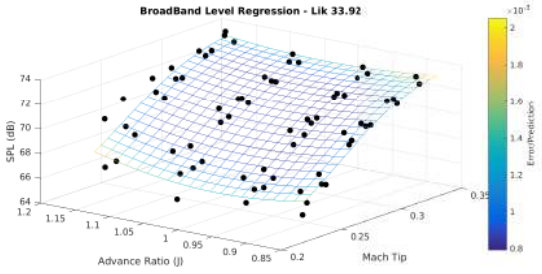

Fig. 7 Kriging regression: J and Tip Mach number effect on broadband level.

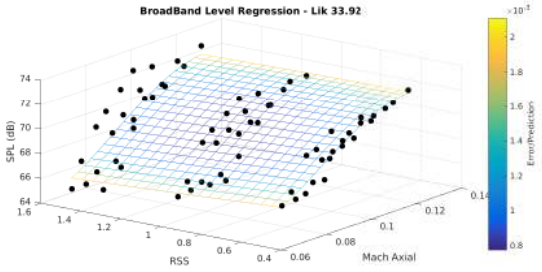

Fig. 8 Kriging regression: RSS and Axial Mach number effect on broadband level.

The conclusion is that the broadband is more flat (smaller decay) when the rotor and stator are far and the speeds are lower, i.e. at high speeds and short rotor-stator spacing the broadband decays rapidly with the frequency.

3.3 Broadband Form Factor

The form factor represents a deformation the linear decay behavior of the broadband noise. If its value is greater than one, the curve bends down for the higher frequencies, and if its value is lower than one, the curve bends up. The next figures (Fig. 12 and Fig. 13) show that the form factor is bigger than one in almost every setup. But higher velocities bring the form factor close to unity and the larger the RSS, the higher the form factor and the scattering of the data.

3.4 Blade Passage Frequency

Fig. 14 shows the first BPF level of the exponential fit for the harmonic orders. It is clear that the first BPF level decrease with the RSS and with Throttle. The behavior with RSS is a conse-

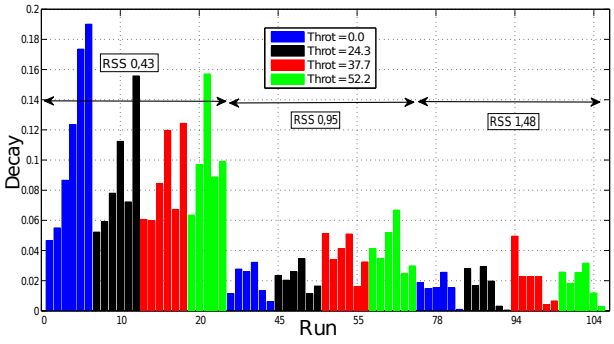

Fig. 9 Broadband decay factor with respect to shaft speed for several configurations.

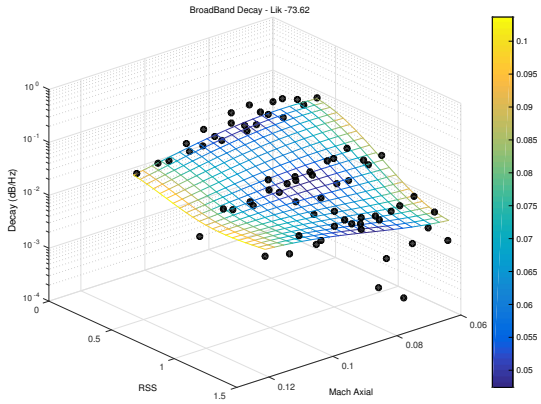

Fig. 10 Kriging regression: RSS and Axial Mach number effect on broadband decay factor.

quence of the form of blade turbulent wake that gets wider with increase of RSS and the velocity deficit lower. The effect of throttle is related with the increase of fan load for bigger blockage of flow on the duct. That increases the amplitude of the periodic forces on the blades and vanes.

The Fig. 15 shows the exponential decay for the BPF. It is clear that the decay increase with RSS and throttle and a soft trend with the decrease of RPM. This relation with RSS, noted on figure, is because the form of blade turbulent wake gets less sharp with the tone order [14]. The relation with throttle can be related with the increase of blade incidence, increasing the boundary layer thickness, and so, the wake width, and the relation with RPM can be related to the axial velocity and the turbulent wake form. For lower RPM the axial speed is lower, for the same throttle, and the wake gets smoother until reach the vane. But a more detailed analysis is required to confirm that hypothesis.

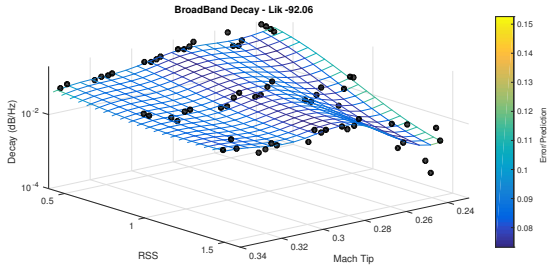

Fig. 11 Kriging regression: RSS and Tip Mach number effect on broadband decay factor.

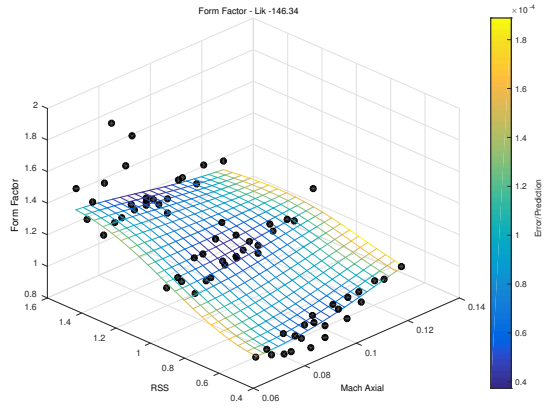

Fig. 12 Kriging regression: RSS and Axial Mach number effect on broadband form factor.

3.5 High Frequency Bubble Analysis

For this analysis the spectra are normalized so that the frequency domain is changed by the shaft order domain on the abscissa axis. The first feature that was observedis that the bubble center is fixed to the 12th BPF, and, apparently, none of the tested parameters are able to change this. Fig. 16 shows an almost linear behavior of the bubble noise level with respect to both axial and tip Mach number. It also shows that throttling shifts the curves up, increasing the level of the bubble, and that RSS has small effects, but also shifting curves up.

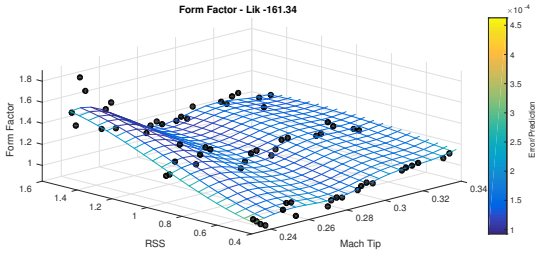

Fig. 13 Kriging regression: RSS and Tip Mach number effect on broadband form factor.

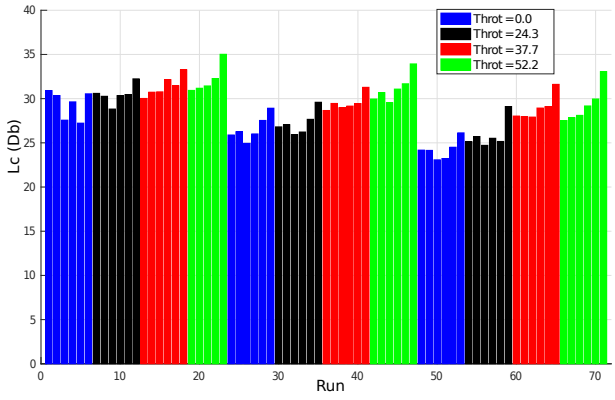

Fig. 14 BPF Level

4 Conclusion

The behavior of the broadband noise can be characterized as a pink noise, i.e. its level decays with frequency increase.

The level of the broadband at the lower frequencies (Lc) depends on the axial Mach number and the advance ratio of the fan. It gets higher when the Mach or the throttling are increased (or advance ratio decreased).

Further, the decay and form factors of the broadband parameterizations are influenced by the geometrical (RSS) and operational (axial Mach) parameters. The higher Mach numbers make the dispersion of the data smaller and, apparently the decay factor less sensitive to rotor-stator spacing. As for the RSS effect, when the rotor and stator are far, the broadband tends to be more flat and when at high speeds and short rotor-stator spacing the broadband decays rapidly with the frequency.

The form factor also showed a good correlation with the RSS. The larger RSS, the higher the

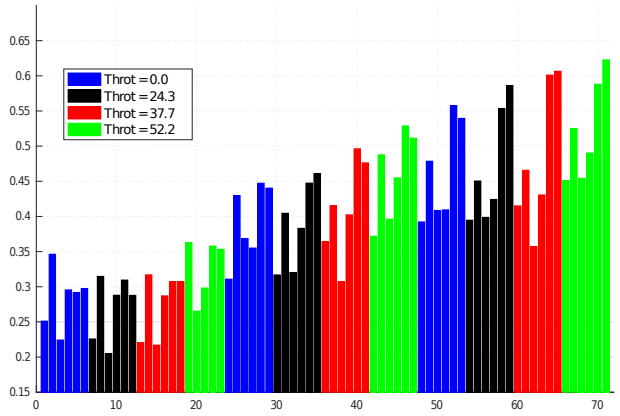

Fig. 15 BPF Decay

form factor. As the frequency goes up, the broadband curve bends down and for the higher RSS configurations, even with flatter curve, the curve bends more abruptly down. Axial Mach number can reduce the influence of the RSS on the form factor.

The use of Kriging regression makes the understanding of the spectral parameter changes easier for the different experiment configurations. The expected error shows that the regression mimics the real surface quite well and points out to further experiments with higher and lower Mach numbers. Some behaviors indicate that there is a need to better adjust the spectra.

The current study provides already a surrogate model for the broadband noise considering the proposed parameterization. The model considers axial Mach number and advance ratio for the broadband level and Mach number and RSS for the decay and form factors.

5 ACKNOWLEDGEMENTS

The authors acknowledgements to CNPq that provided the grant during the PHD, Finep that provided the resources for the Rig construction and Embraer for the colaboration.

References

[1] D. Werner, “Almost 40 years of airframe noise research: What did we achieve?,” *Journal of Aircraft*, pp. 353–367, 2010.

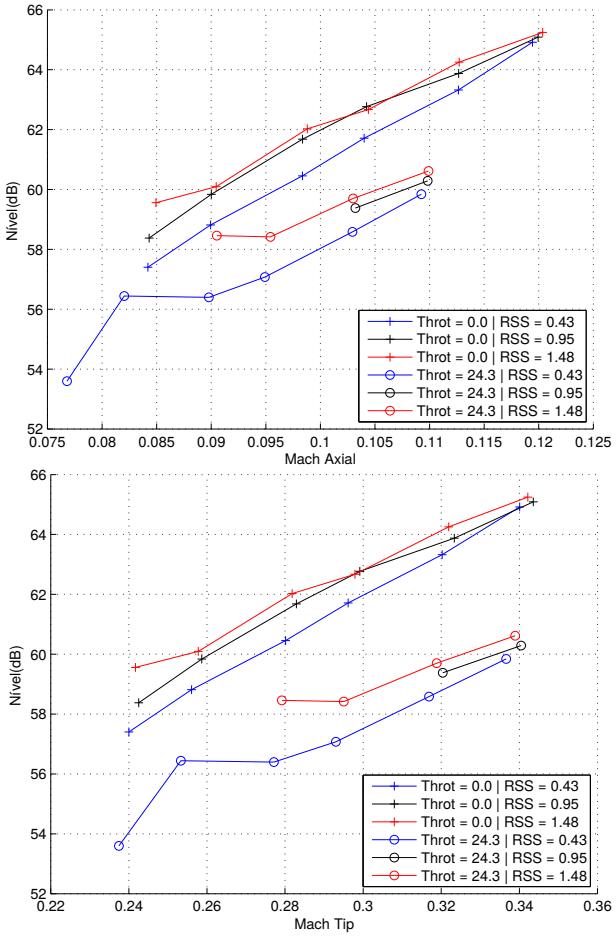

Fig. 16 High frequency bubble with respect to blade Machs number

[2] D. Casalino, F. Diozzi, R. Sannino, and A. Paonessa, "Aircraft noise reduction technologies: A bibliographic review," *Aerospace Science and Technology.*, pp. 1–17, 2008.

[3] D. Sutliff, "Rotating rake turbofan duct mode," Tech. Rep. NASA/TM2005-213828, NASA, 2005.

[4] K. Tanigawa, N. Yamasaki, and T. Ooishi, "Improved hybrid prediction of fan noise," in *Proceeding of 15th AIAA/CEAS Aeroacoustics Conference (30th AIAA Aeroacoustics Conference)*, 2009.

[5] L. Enghardt, L. Neuhaus, and C. Lowis, "Broadband sound power determination in flow ducts," *Proceeding on 10th AIAA/CEAS Aeroacoustics Conference*, 2004.

[6] J. M. Tyler and T. G. Sofrin, "Axial flow compressor noise studies.," in *Proceeding on S.A.E. aeronaut. meeting,*, 1961.

[7] Y. Wu, G. Jin, H. Ouyang, and Z. Du, "Experimental investigations on tip leakage flow and noise in skewed blades," in *Proceeding on IAA/CEAS Aeroacoustics Conference*, no. AIAA 2010-3908, 2010.

[8] A. B. Nagy, "Aeroacoustics research in europe: The ceas-asc report on 2010 highlights," *Journal of Sound and Vibration*, 2010.

[9] T. Marotta and B. Schuster, "A comparison of fan inlet dynamic wall pressure measurements from rig and engine tests," in *Proceeding on 18th AIAA/CEAS Aeroacoustics Conference (33rd AIAA Aeroacoustics Conference)*, no. AIAA 2012-2271, 2012.

[10] L. C. Caldas, "In-duct beamforming and mode detection using a circular microphone array for the characterisation of broadband aeroengine fan noise," Master's thesis, Escola Politécnica da Universidade de São Paulo, São Paulo-Brasil, 2016.

[11] ISO, "Acoustics - determination of sound power radiated into a duct by fan and other air-moving devices - induct method," ISO 5136:2003, International Organization for Standardization, Geneva, Switzerland, 2003.

[12] D. G. Krige, "A statistical approach to some basic mine valuation problems on the witwatersrand," in *Journal of the Chemical, Metallurgical and Mining Engineering Society of South Africa*, vol. 52, 1951.

[13] J. Richard F. Bozak, "Advanced noise control fan aerodynamic performance," Tech. Rep. NASA/TM 2009-215807, NASA, 2009.

[14] M. Goldstein, *Aeroacoustics*. McGraw-Hill International Book Co., 1976.

6 Contact Author Email Address

To contact the authors, please mailto:
rafael.cuenca@ufsc.br (Cuenca, R. G.)
pgreco@sc.usp.br (Greco, P. C.)
bernardo.rocamora@gmail.com (Rocamora, B. M.)

Copyright Statement